LPV modeling and LFT Uncertainty Identification for Robust Analysis: application to the VEGA Launcher during Atmospheric Phase ⋆

Andres Marcos * **Samir Bennani** ** **Christophe Roux** *** **Monica Valli** ***

* *University of Bristol, BS8 1TR, United Kingdom (andres.marcos@bristol.ac.uk).*
** *ESA-ESTEC, Noordwijk, 2201AZ, The Netherlands (e-mail: samir.bennani@esa.int)*
*** *ELV, Rome, 00034, Italy (e-mail: Christophe.Roux@elv.it, Monica.Valli@consultant.elv.it)*

Abstract: In this article, the development of a proper Linear Fractional Transformation model for the robust analysis of the atmospheric controllers of the European VEGA launcher is presented. By proper it is meant a model that: (i) captures the key launcher's behavior during the ascent atmospheric phase, (ii) has a complexity in terms of number of parameters and repetitions that does not limit the applicability of robust analyses, (iii) can be easily updated with very different trajectory profiles, and (iv) arises from a methodology that is well connected with industrial practice and can be understood and used relatively easy. This last requirement is fundamental to transfer the LFT methodology into the VEGA program, which is critical if robust analysis is to be used within their verification and validation process. The potential of the proposed methodology and the validity of the developed LFT models for robust analysis have been successfully verified using simulation data from three of the four VEGA qualification flights.

Keywords: LFT modeling, robust analysis, flexible launcher

1. INTRODUCTION

A concept widely used in robust control is the structured singular value μ, which analytically evaluates the robustness of uncertain systems Doyle, J. et al. (1991). A key aspect on the application of μ is the development of a proper Linear Fractional Transformation (LFT) model. By proper it is meant a model that captures the critical parametric behavior of the nonlinear system under consideration within a complexity that still enables the application of the μ analysis algorithms Balas, G.J. et al. (1998).

The use of these concepts, methods and tools is quite consolidated and nowadays is ingrained in those industrial groups that had the opportunity and interest in learning them. For example, for satellites see references Charbonnel, C. (2010) and Pittet, C. and Arzelier, D. (2006), and for their use on the European Automated Transfer Vehicle (ATV) see Ganet-Schoeller, M. et al. (2009). Nevertheless, transferring these methods to other industrial groups is still difficult, and despite well document manuals, tutorials and many publications, there is always the need of demonstrating the techniques' potential through tailored-made simplified study cases, as well as through application to a relatively sophisticated benchmark of the system under consideration.

An example of the potential difficulties of transferring these methods to a launcher programme can be seen in Jang, J.W. et al. (2008). In that reference a simple mass-spring-damper case was used to illustrate the "limitations" of μ in evaluating its potential for the Ares I programme. It was claimed that μ suffered of conservativeness and had to be used with care even for that simple case. But actually, it can be shown that if a proper LFT model is used then μ correctly identifies a worst-case right on the stability boundary of the (damping, spring) coefficients plane. Since the authors were key control experts in the Ares I programme, their conclusions probably carried quite a weight in accepting or sidelining the use of μ within their verification and validation (V&V) process.

Thus, this article aims to evince that LFT modeling can be used very effectively and efficiently to obtain a proper LFT model that includes the key behavior of a launcher during atmospheric phase, and thus can be used subsequently for robust analysis of the launcher's controllers. The methodology developed reconciles the standard examination of the analytical representation of the system with the identification of uncertainty models and variability levels based on time-data obtained from a high-fidelity, nonlinear simulator. The proposed method has been applied to the European VEGA launcher during its ascent atmospheric phase, and the obtained LFT models were successfully used subsequently by μ analysis to identify parameter combinations that had to be examined by the VEGA control design group as potential problematic issues.

The layout of the article is as follows: first, the VEGA launcher and mission are presented, including a detailed derivation of the equations of motion applicable to the benchmark. Then, the LFT modeling and uncertainty identification methodology is presented. It follows a step-by-step description of the application to the VEGA launcher prior to the conclusions.

⋆ This work was funded by ESA-ESTEC Contract No. 4000111052/14/NL/GLC/al within the project "Analytic Stochastic Time Varying Mu Analysis for the VEGA GNC"

2. VEGA LAUNCHER AND BENCHMARK

2.1 VEGA launcher and mission

VEGA, see Figure 1, is the new European Small Launch Vehicle developed under the responsibility of ESA by ELV as prime contractor. The launcher successfully performed a maiden launch at the beginning of 2012 from the Centre Spatial Guyanais in Kourou and three more qualifications flight since, the 4^{th} flight on 11^{th} February 2015.

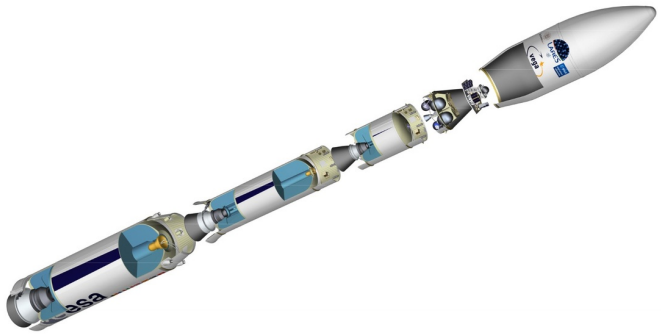

Fig. 1. VEGA launcher in LARES mission configuration

VEGA follows a four-stage approach formed by three solid propellant motors (P80, Zefiro 23 and Zefiro 9) providing thrust for the 1^{st}, 2^{nd} and 3^{rd} stages; and, a bi-propellant liquid engine (LPS) on the 4^{th} stage. All stages are controlled via a thrust vectoring system (TVC). There is also a Roll and Attitude Control System (RACS) performing 3-axes control during the ballistic phase and roll rate control during the propelled phases.

2.2 VEGA high-fidelity simulators and mission

The official high-fidelity, non-linear simulator used in the VEGA program for all GNC verification and validation is called VEGAMATH. This simulator is characterized by:

- High-fidelity 6 Degrees-of-Freedom motion
- Tail-Wag-Dog effects
- Bending and sloshing modes
- Full external environment (rotating Earth, winds...)
- Disturbances (torques at separation, bias, offsets)
- Nonlinear aerodynamics (incl. aero-elastic effects)
- TVC system (including computing delays, backlash, bias)
- Full representative code implementing the actual Guidance, navigation and control (GNC) system
- Propulsion and mass-center-inertia (MCI) properties
- Detailed inertial navigation system (INS)
- Detailed RACS models (with thermal & thrust dynamics, filters, quantization, noise...)

VEGAMATH cannot be distributed due to proprietary reasons, thus another simulator called VEGACONTROL was provided with most sub-systems as black-boxes, see Figure 2. The main differences with the official one are that it simulates only the 1^{st} atmospheric phase of VEGA (i.e. P80) and it is prepared for accelerated-time simulation (through protected and compiled code). Note that it retains most of the VEGAMATH sophistication, including bending/sloshing modes, RACS model, wind-scaling profiles, and enhanced correlation of key parameters.

Both simulators allow modifying the scattering values (uncertainties and dispersions) of up to 125 different parameters,

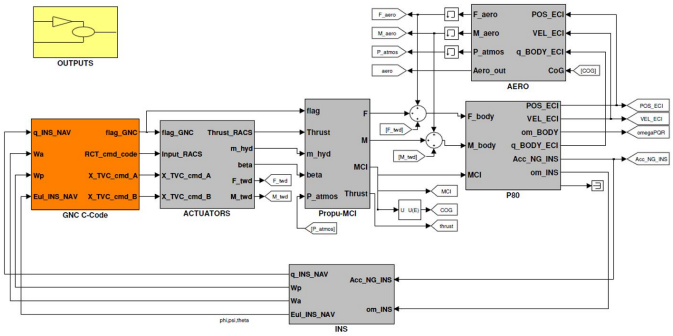

Fig. 2. VEGACONTROL Simulink implementation

including MCI, aerodynamics, wind profiles, INS mounting and thrust among others. Each scattering variable is represented by a normalized "flag" parameter (i.e. ranging between $[-1, 1]$ with the zero value indicating nominal behaviour).

In terms of the VEGA mission used for the work in this article, Figure 3 shows the nominal flight profiles for altitude, Mach and dynamic pressure times angle ($Q * \alpha$), which is a specifically critical measure for launchers as it provides an indication of the experimented loads –the upper bound indicates its limit. In addition, it is noted that the approach presented in this article had already being applied to two previous missions: one for the release of the LARES satellite, i.e. VEGA's maiden flight, and another called DT1 and characterized by minimum mass and inertia (but that turned out to be very sizing for the GNC performance). The missions are quite different, each with a substantially different payload, trajectory profile, and as typical for launchers with a specifically tuned controller.

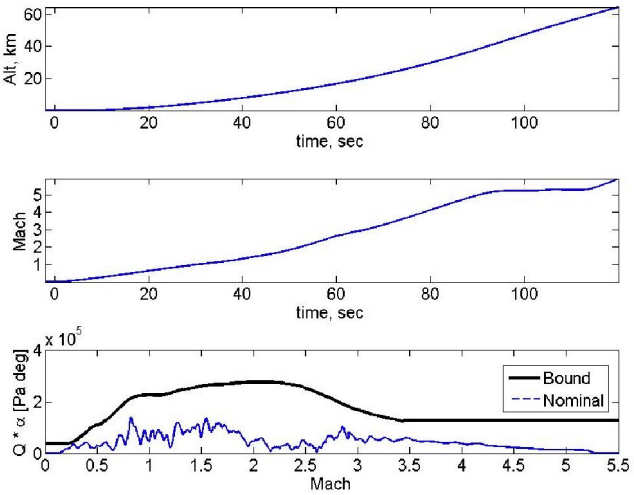

Fig. 3. VEGA mission profile: altitude, Mach and $Q\alpha$

2.3 VEGA equations of motion

Orr, J.S. et al. (2009) details the equations of motion for a flexible launcher in a clear state-space format showing the uncoupled and coupled effects for the three main contributors: rigid, flexible and sloshing. In this article this reference is followed, but focusing on the yaw motion with flexible effects, and using a notation more agreeable to aeronautical standards, i.e. yaw plane and associated angle are defined as the XY-plane and sideslip angle β respectively.

For any launcher vehicle, its yaw or pitch dynamics are completely described by its attitude (yaw ψ or pitch θ) and linear motion (y or z) in a frame linked to the trajectory velocity, see Figure 4. For axis-symmetric launchers, both motions are identical

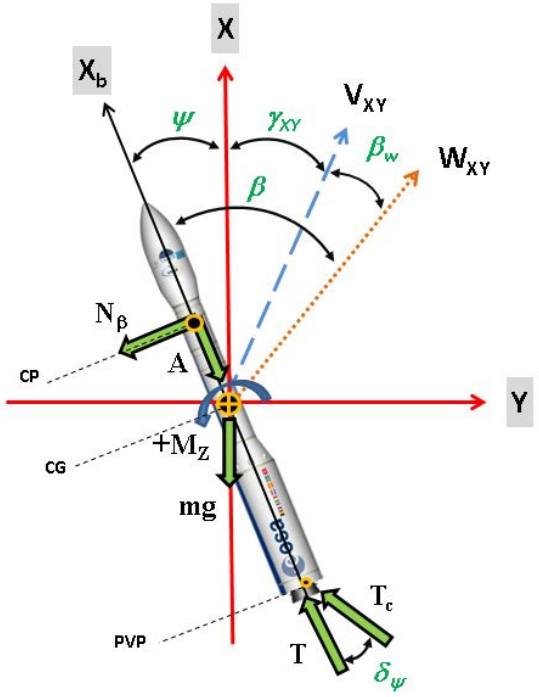

Fig. 4. VEGA yaw-motion diagram

The trajectory's total angular acceleration $\ddot{\psi}$ and linear acceleration $\ddot{y}$ are expressed as the sum of the rigid and flexible forces and moments (with m mass and J_{yy} moment of inertia):

$$m\ddot{y} = F_r + F_f \qquad J_{yy}\ddot{\psi} = M_r + M_f \tag{1}$$

The rigid-motion force F_r and moment M_r are given by (using short-hand for the cosine $c_\#$ and sine $s_\#$ functions):

$$\begin{aligned} F_r &= As_\psi - N_\beta c_\psi - Ts_\psi - T_c(c_{\delta_\psi}s_\psi + s_{\delta_\psi}c_\psi) \\ M_r &= N_\beta(x_{CP} - x_{CG}) - T_c s_{\delta_\psi}(x_{CG} - x_{PVP}) \end{aligned} \tag{2}$$

where A is axial force, $N_\beta = N\beta$ is the normal force in the XY-plane, (T, T_c) are respectively ungimballed and gimballed thrust, (x_{CG}, x_{CP}, x_{PVP}) are the x-coordinates for center of gravity, center of pressure and TVC pivot-point. The sideslip angle is defined as $\beta = \psi + (\dot{y} + x_{CP}\dot{\psi})/V$ assuming that the angle is computed locally at the CP and there is no wind (W_{XY}=0). The Lift coefficient is given by $N = Q\,S_{ref}C_{N\beta}$, where the latter term is the lift gradient in the XY-plane, S_{ref} the launcher surface reference and Q the dynamic pressure.

Using small-angle approximations, total force $F = T + T_c$, $\bar{x}_{CP} = (x_{CP} - x_{CG})$ and $\bar{x}_{CG} = (x_{CG} - x_{PVP})$:

$$\begin{aligned} F_r &= -(F-A)\psi - N\psi - N\frac{\dot{Y}}{V_{rel}} - T_c\delta_\psi \\ M_r &= N\bar{x}_{CP}\psi + N\bar{x}_{CP}\frac{\dot{Y}}{V_{rel}} - T_c\bar{x}_{CG}\delta_\psi \end{aligned} \tag{3}$$

Next, the flexible forces and moments are considered:

$$\begin{aligned} F_f &= T_c\sum_{i=1}^{k} RMC_{PVP_i}\, q_i \\ M_f &= -T_c(\bar{x}_{CG}\sum_{i=1}^{k} RMC_{PVP_i} + \sum_{i=1}^{k} TMC_{PVP_i})\, q_i \end{aligned} \tag{4}$$

where TMC_{PVP_i} and RMC_{PVP_i} are the i^{th} bending mode translational and rotational lengths at pivot point (PVP) –as opposed to at the inertial navigation system (INS) for the output equations, see C-matrix in equation 6. The flexible dynamics are given based on a free-free beam model with orthogonal bending modes q_i represented as 2^{nd} order model with frequency ω_{iB} and damping ζ_{iB}:

$$\ddot{q}_i + 2\zeta_{iB}\omega_{iB}\dot{q}_i + \omega_{iB}^2 q_i = -T_c\, TMC_{PVP}\,\delta_\psi \tag{5}$$

Adding up all the contributions and using 2 bending modes, the dynamic equations can be expressed in state-space format using four rigid states $(y, \dot{y}, \psi, \dot{\psi})$, four flexible states $(q_1, q_2, \dot{q}_1, \dot{q}_2)$, three outputs $(\psi, \dot{y}, y)$ and one input (δ_ψ) as:

$$A = \left[\begin{array}{c|c} A_r & A_{rf} \\ \hline A_{fr} & A_f \end{array}\right] \qquad B = \left[\begin{array}{c} B_r \\ \hline B_f \end{array}\right] \qquad C = [\,C_f \,|\, C_f\,]$$

$$A = \left[\begin{array}{cccc|cc} 0 & 1 & 0 & 0 & 0_{1q} & 0_{1q} \\ 0 & a_1 & a_2 & a_3 & a_{zq} & 0_{1q} \\ 0 & 0 & 0 & 1 & 0_q & 0_{1q} \\ 0 & a_4 & A_6 & a_5 & a_{\psi q} & 0_{1q} \\ \hline 0_{q1} & 0_{q1} & 0_{q1} & 0_{q1} & 0_{qq} & I_q \\ 0_{q1} & 0_{q1} & 0_{q1} & 0_{q1} & A_{qq} & A_{q\dot{q}} \end{array}\right] \qquad B = \left[\begin{array}{c} 0 \\ a_p \\ 0 \\ K_1 \\ \hline 0_{q1} \\ a_{qk1} \end{array}\right] \tag{6}$$

$$C = \left[\begin{array}{cccc|cc} 0 & 0 & 1 & 0 & -RMC_{INS} & 0_{1q} \\ 0 & 1 & 0 & a_Z & 0_{1q} & TMC_{INS} \\ 1 & 0 & a_Z & 0 & TMC_{INS} & 0_{1q} \end{array}\right] \qquad D = \begin{bmatrix} 0 \\ 0 \\ 0 \end{bmatrix}$$

where 0_{1q}, 0_{q1}, 0_{qq} and I_q are zero and unit matrices of appropriate order (based on the number of modes used). Notice that the matrix A is rank deficient in this formulation since the displacement y is used as a state without any dynamics from a sensor model. This is not an issue, since it is possible to remove the channel and use the integrated velocity signal in the output, and in any case during the LFT process any unobservable and uncontrollable channel is removed.

The corresponding matrix coefficients are given by:

$$\begin{aligned} &v_\beta = -N\frac{\bar{x}_{CP}}{J_{yy}}; \qquad acc = \frac{F-A}{m}; \\ &a_1 = -N\frac{1}{m}\frac{1}{V_{rel}}; \quad a_2 = -a_1\bar{x}_{CP}; \quad a_3 = -acc + a_1 V_{rel} \\ &a_4 = -v_\beta\frac{1}{V_{rel}}; \qquad A_6 = a_4 V_{rel}; \qquad a_5 = -a_4\bar{x}_{CP} \\ &a_Z = x_{CoG} - x_{INS}; \quad a_P = -\frac{T_c}{m}; \quad K_1 = -\frac{T_c}{J_{yy}}\bar{x}_{CG} \\ &a_{zq_i} = \frac{T_c}{m}RMC_{PVP_i}; \; a_{\psi q_i} = \frac{T_c}{J_{zz}}(RMC_{PVP_i}\bar{x}_{CG} + TMC_{PVP_i}) \\ &A_{qq_i} = -\omega_{iB}^2; \; A_{q\dot{q}_i} = -2\zeta_{iB}\omega_{iB}; \\ &a_{zq} = [a_{zq_1} \;\; a_{zq_2}] \qquad a_{\psi q} = [a_{\psi q_1} \;\; a_{\psi q_2}] \\ &A_{qq} = diag(A_{qq_1}, A_{qq_2}) \qquad A_{q\dot{q}} = diag(A_{q\dot{q}_1}, A_{q\dot{q}_2}) \\ &a_{qk1_i} = -T_c\, TMC_{INS} \qquad a_{qk1} = [a_{qk1_1} \;\; a_{qk1_2}]^T \end{aligned} \tag{7}$$

All the launcher variables can be represented as depending on time t or on non-gravitational speed, VNG. All these variables can be used to derive an LFT/LPV model, see Section 3.3.1 for details on the specific choice used in this work. The launcher dynamic model given in equation 6 captures the main characteristics of the 1^{st} atmospheric phase (P80) and is typically used to design the launchers' controllers for this phase.

3. LFT MODELING AND UNCERTAINTY IDENTIFICATION METHODOLOGY

In this section, a cursory presentation of the main theoretical concepts for LFT and μ is given first, the latter is provided since the purpose of the LFT model is mostly for robust analysis (and design). Then, a discussion on the main LFT modeling choices and their effect is given followed by the proposed methodology.

3.1 Robust analysis: Linear Fractional Transformations and μ

A LFT is a representation of a system using a feedback interconnection and two matrix operators, $M = [M_{11}\ M_{11};\ M_{11}\ M_{11}]$ and Δ. The matrix M represents the nominal (known) part of the system while Δ contains the unknown, time-varying or uncertain parameters $\rho_i(t)$. There are two possible types of LFTs: lower and upper (see Fig. 5).

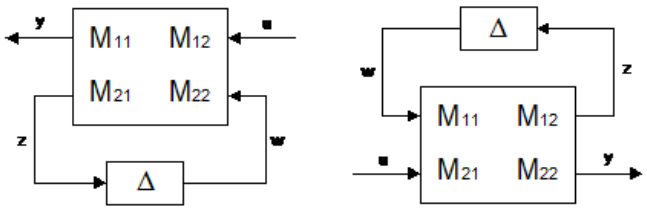

Fig. 5. Lower and upper LFTs

The matrix Δ is unrestricted in form (structured or unstructured) or type (nonlinear, time-varying or constant). It is important to note that unstructured uncertainty at component level becomes structured at system level. The selection and uncertain modeling of the variable set $\rho(t) \in \Delta$ that captures the behavior of the nonlinear system is a task that is not always obvious a priori. Indeed, this step is key to obtain a reliable LFT that will yield relevant and meaningful results and, despite its apparent simplicity, is where most of the LFT modeling effort is concentrated. There are several approaches that can be used to obtain a reliable LFT model (see Lambrechts, P. et al. (1993); Magni, J.F. (2004); Marcos, A. et al. (2007) and references therein).

3.2 LFT modeling choices and their effect

The proposed LFT methodology reconciles the standard examination of a system analytical representation with the identification of uncertainty models and variability levels based on simulated time-data. Thus, it is founded on the availability of a mathematical, analytical model of the system as well as of a high-fidelity, nonlinear simulator (but not necessary visible to the LFT modeling engineer, i.e. black-box). It is noted that these two requirements are typically available for most industrial control design projects.

Before presenting the approach, the four main choices for any LFT modeling process are listed:

(1) *Type of uncertain parameters,* Δ_x: non-physical, physical or constituent. The first term relates to parameters, fictitious or otherwise, that are mathematical in nature and not directly related to a single physical parameter. For example, one of the matrix coefficients in equation 6 is given by the aerodynamic parameter A_6 and contains the effects from several other physical parameters, i.e. $A_6 = N\bar{x}_{CP}/J_{yy}$. One of these physical parameters, the lift coefficient N, can also be expressed in turn based on a subset of physical constituent parameters, $N = Q\,S_{ref}C_N/\beta$. Thus, the term constituent can be defined as those physical variables that are also directly responsible for the uncertainty in other parameters.

(2) *Type of LFT model*: multiplicative $x = x_0(1+\sigma_x\Delta_x)$, additive $x = x_0 + \sigma_x\Delta_x$, or inverse $x = x_0(1+\sigma_x\Delta_x)^{-1}$; Note that some models are equivalent from a mathematical perspective, i.e. additive and multiplicative, but that the actual implementation will change the character of the LFT model, and thus of the analysis results.

(3) *Level of uncertainty,* σ_x: range of the uncertainty, chosen from experience, approximation or data-analysis;

(4) *Correlation of the uncertain parameters*: as shown before, most physical parameters tend to be correlated to a basis set of other physical parameters (which we termed constituents). Even if the most constituent dependence is not used (as it may yield very high LFT dimension by the sheer number of repetitions of the constituent parameters), some level of correlation should be attempted in order to avoid correlated uncertainty changing in complete independent manner, and thus resulting in non-physical system behavior. For example, the mass and moment of inertia of a launcher will change coordinately as the fuel is burnt (i.e. the more fuel is consumed, the less mass there is and the moment changes accordingly). The complex dependency underlying the mass, moment of inertia and fuel burning can be easily captured using either the physical constituent parameter, fuel burning ratio δ_{Tc}, or a non-physical parameter that reflects the correlated changes.

The importance of using more physical and correlated LFT models cannot be understated since a simpler uncertainty set may result in an easier to get LFT model, and of smaller dimension, but at the expense of resulting in an over-bounded parameter space. The effect of having such an over bounded space is negative from the dual perspectives of:

(1) *Design*, since the designer must ensure satisfaction of objectives for the selected parameter space region. And thus, if it is much larger than the actual system behavior then the controller will need to have stronger (than necessary) robustness properties in detriment of performance.

(2) *Analysis*, since depending on the system and the type of analysis (i.e. LTI eigenvalue or gain/phase margin), more effort and time must be spent analyzing the larger space, thus leading to conservative or even void analysis results (e.g. in μ robust analysis, bounds impossibly apart).

3.3 LFT modeling and uncertainty identification process

The proposed process follows three distinct steps:

3.3.1 System Examination

The goal of this step is to find: (i) the largest set Ω_{sys} of system parameters representing the behavior of the system, (ii) the smallest set Ω_Δ of uncertain parameters that can be varied by the designer and are connected to Ω_{sys} , and (iii) the smallest number of time simulations $(y(t),u(t))_i = 1,...p$ such that the individual and group effects of the parameters in Ω_Δ are adequately examined by analyzing their effects on Ω_{sys}. Note that optimal terms such as minimal and maximal are not used due to the practical impossibility of guaranteeing the optimality.

This goal is accomplished by examining:

A. Analytical system (linear). The ordinary differential equations (ODEs) representing the system's equations of motion as well as their linearized counterparts, e.g. state-space matrices, are examined to extract into the set Ω_{sys} all the relevant system parameters. The priority is to choose physical parameters, as they are easier to analyze, but mathematical parameters clearly condensing the effect of some of these physical variables can also be included in the set. For example, from examination of equation 7 it is easy to see (the coefficients have been written with this goal in mind) that N affects all the rigid coefficients (through ν_β) but that a_1 and a_4 can also be used as a choice as they affect respectively (a_2, a_3) and (a_5, A_6). The populating of Ω_{sys} can be as straight forward as picking out all the parameters present in the ODEs or in the state-space coefficients. But system knowledge can, and should, also be used to exploit system structure. Note, that all the parameters in Ω_{sys} must be available, or be calculated, from the measurements $y(t)$. For the VEGA P80, the rigid, flexible and mathematical subsets are:

$$\begin{aligned}\Omega_{sys-RIG} &= \{m, J_{yy}, T_c, V_{rel}, x_{CG}, x_{CP}, Q, C_N, acc, \beta\}\\ \Omega_{sys-FLX} &= \{\omega_{iB}, TMC_{PVP_i}, RMC_{PVP_i}\}\ _{i=1,2}\\ \Omega_{sys-MTH} &= \{N, \nu_{beta}, a_1, a_4, A_6, K_1\}\end{aligned} \tag{8}$$

Subsequently, the set Ω_Δ is populated with uncertain parameters known, or with potential, to affect the parameters in Ω_{sys}. The departure point is the list of the uncertainty flags available in the highest-fidelity, nonlinear simulator $\Omega_{flags} = \{\delta_\#\}$. Note that the dimension of Ω_Δ has a direct effect on the number of simulations that will be required, thus it should be kept as small as possible based on the knowledge of the physics of the system (especially in cases as VEGACONTROL that has 125 flags):

$$\begin{aligned}\Omega_{\Delta-RIG} = \{&\delta_m, \delta_{J_{yy}}, \delta_{x_{CG}}, \delta_{x_{CP-DSP}}, \delta_{x_{CP-UNC}}, \dots\\ &\delta_{C_N-DSP}, \delta_{C_N-UNC}, \delta_{ISP}, \delta_{Tc}, \delta_\rho\}\\ \Omega_{\Delta-FLX} = \{&\delta_{\omega_B}, \delta_{TMC_{PVP}}, \delta_{RMC_{PVP}}, \delta_{TMC_{INS}}, \delta_{RMC_{INS}}\}\end{aligned} \tag{9}$$

where δ_{ISP} is the specific impulse, and $(\delta_{\#-DSP}, \delta_{\#-UNC})$ indicate a parameter determined by dispersions and uncertainty constants, see Roux, C. and Cruciani, I. (2008).

Note that if time-varying parameters are included in Ω_Δ, e.g. rotational velocity VNG, and all the subsequents steps are followed, the result will be an LPV model in LFT format.

B. Simulation data-analysis (nonlinear) Once the sets Ω_{sys} and (especially) Ω_Δ are identified, time-domain simulations using the nonlinear simulator must be performed. The number of simulations is given by $p = n \times m \times k$, where $n = dim(\Omega_\Delta)$ and m and k are the number of grid points used respectively to set iteratively each parameter in Ω_Δ at m_i while setting all other uncertainty flags in the simulator to the same value k_j.
For the VEGA case, $n = dim(\Omega_{\Delta-RIG}) + dim(\Omega_{\Delta-FLX}) = 16$, and a minimal set of runs is performed by choosing the grids as the minimum, nominal and maximum value of the flags, i.e. m=k=[-1, 0, +1]. This yields $p = 16 \times 3 \times 3 = 144$ simulations, but after a first examination 4 more sets were added to Ω_Δ to test groupings of parameters for a total of 180 simulations.

3.3.2 Uncertainty Identification

The goals in this step are to: [1] reduce the sets Ω_Δ and Ω_{sys}, by analyzing the effects of the former on the later using the simulation data $(y(t), u(t))_i = 1, \dots 180$, and then [2] identify the most appropriate structure and data for the final $\Omega_{sys}(\Omega_\Delta)$, e.g.:

$$\tau = \tau_0 + \sigma_\tau^a \delta_\tau^a + \sigma_\tau^b \delta_\tau^b + \sigma_\tau^c \delta_\tau^a \delta_\tau^b \dots \tag{10}$$

where $\tau \in \Omega_{sys}$, $(\delta_\tau^a, \delta_\tau^b \dots) \in \Omega_\Delta$ and $(\tau_0, \sigma_\tau^a, \sigma_\tau^b, \sigma_\tau^c \dots)$ represent the calculated nominal and uncertainty levels for τ.

In achieving these goals is of paramount importance to apply engineering judgement to minimize the amount of data to analyze (or be capable to handle in a semi-automated fashion the identification process). A proper visualization of the results is thus found to be key to rationalize the data analysis.

In the present case, it was opted to automatically generate three sets of two figures, one with 14 plots for the rigid parameters (the 10 physical parameters in $\Omega_{sys-RIG}$ plus 4 other parameters known to be important, such as $Q\alpha$) and another with 16 plots providing the responses for the first 4 bending modes and their derivatives $(q_i, \dot{q}_i)$. The plots in each figure contain three responses, one for each of the $m = [-1, 0, +1]$ of the Ω_Δ parameter tested, and each of the three 2-figures sets is obtained by setting all the other flags at respectively $k = [-1, 0, +1]$. Thus, the 180 simulations can be "easily" visualized in 20 sets of 2-figures (one for rigig and the other for bending).

As an example, Fig. 6 shows the effect of the flag δ_{Tc} (burnt time) on the set of rigid variables.The figure shows the results for δ_{Tc}=[-1, 0, 1] with all other flags set at k=-1. The impact of this parameter on the launcher dynamics is apparent, which indicates that likely it is one of the variables to take into account in the search for worst-cases (this also coincides with the physics knowledge on the launcher). For ease of comparison, the Q parameter is shown in Fig 7 for the variations in δ_{Tc} (top) and δ_m (bottom) –each column for a value of k. Note that it is immediately seen that the latter has no effect while the former has a similar linear effect across k.

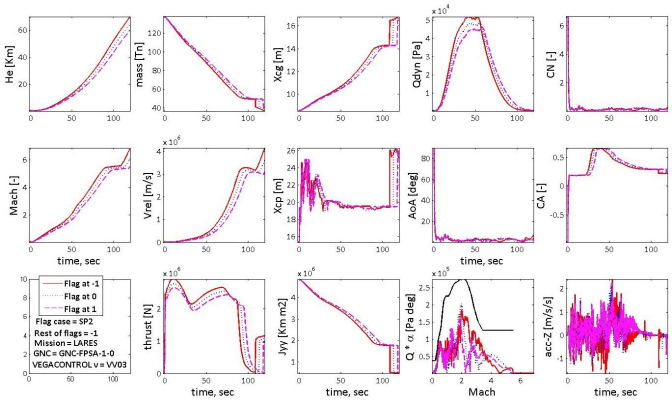

Fig. 6. VGCTRL time responses for δ_{Tc}=[-1, 0, 1] and k=[-1]

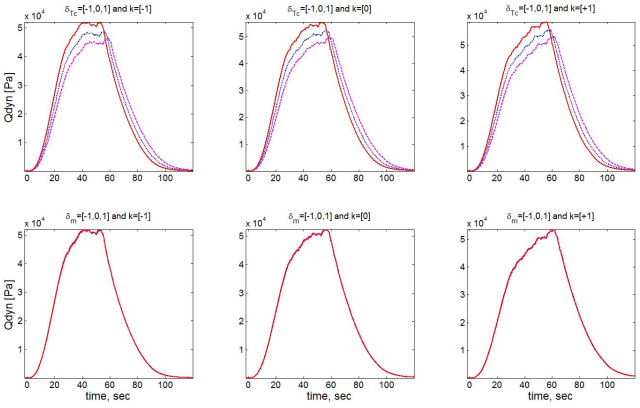

Fig. 7. VGCTRL time responses for δ_{Tc} (top) and δ_m (bottom)

As aforementioned, the first goal is to identify a reduced combination of uncertain and system parameters that account for the most changes with respect to the nominal flight. The potential bad extremes are to select: (i) many system variables and many uncertain parameters, (ii) many system variables but insufficient number of uncertain parameters, (iii) many uncertain parameters but insufficient system variables, and (iv) insufficient number of system and uncertain parameters.

From the visual inspection of the 20 sets of 2-figures, it was determined that all the parameters in $\{\Omega_{sys-RIG} \cup \Omega_{sys-FLX}\}$, except for the angle β, will be considered as dependent on uncertainty. Thus, the uncertain physical set $\tau(\delta_\tau^\#)$ has dimension 14 (using 2 bending modes), while $\delta_\tau^\#$ is given by:

$$\begin{aligned}\delta_\tau^\# = \{&\delta_{Tc}, \delta_\rho, \delta_{x_{CP-DSP}}, \delta_{x_{CP-UNC}}, \delta_{C_{N-DSP}}, \delta_{C_{N-UNC}}, \cdots \\ &\delta_{\omega_B}, \delta_{TMC_{PVP}}, \delta_{RMC_{PVP}}, \delta_{TMC_{INS}}, \delta_{RMC_{INS}}\}\end{aligned} \tag{11}$$

This down-selection leads to the last goal of this step of representing the set $\tau(\delta_\tau^\#)$ as polynomials in $(\delta_\tau^\#, \tau_0, \sigma_\tau^\#)$, i.e. choosing the structure (uncertain model type) and obtaining the associated data (nominal values and uncertainty variability levels).

To find the structure essentially means to asses the correlation between the system variables in τ and the uncertain parameters in $\delta_\tau^\#$, as well as the cross-correlation between system parameters (or between uncertain parameters). The key idea is to use simple structures first, and increment the complexity as required. Indeed, always start with a linear structure (a one-to-one dependency between system and uncertain parameters) and/or bilinear (when a system variable is influenced by two uncertain parameters) before trying higher-order dependencies. For ease of identification the additive LFT model type is preferred, especially if the dependency is on several uncertain parameters.

For VEGA, and based also on the observed trends from the visual data-analysis (plus numerical tests to ensure the error in the identification is within acceptable limits), only linear and bilinear polynomial fits were used. For example,

$$\begin{aligned} x_{CG} &= x_{CG_0} + \sigma_{x_{CG}}^{\delta_{Tc}}\ \delta_{Tc} \qquad T_c = T_{c_0} + \sigma_{T_c}^{\delta_{Tc}}\ \delta_{Tc} \\ x_{CP} &= x_{CP_0} + \sigma_{x_{CP}}^{CP_{DPS}}\ \delta_{x_{CP-DSP}} + \sigma_{x_{CP}}^{CP_{UNC}}\ \delta_{x_{CP-UNC}} \\ Q &= Q_0 + \sigma_Q^{\delta_{Tc}}\ \delta_{Tc} + \sigma_Q^{\delta_\rho}\ \delta_\rho \end{aligned} \tag{12}$$

And the nominal τ_0 and uncertainty level $\sigma_\tau^\#$ values are directly obtained numerically by calculating respectively the mean and maximum modulo standard deviation of the time responses for the minimum, nominal, maximum of the δ_τ=[-1, 0, +1].

3.3.3 LFT Modeling

The final step is to introduce all the obtained polynomial functions (one per selected system variable and each dependent on one or several of the selected uncertain parameters) into the state-space formulation of the system and then transform the resulting polynomial matrix into an LFT model. This step is not treated in detail as there are several toolboxes available to perform it automatically – see Balas, G.J. et al. (1998); Magni, J.F. (2004); Marcos, A. et al. (2007); Szabo, Z. et al. (2011).

The final LFT model has 11 uncertain parameters (eq. 11) and a total order of 37, i.e. most parameters repeated 2 or 3 times except for δ_{Tc} which is present 11 times. This model, or others similarly derived, has been used to analyze the robust performance and stability of the VEGA controllers for the 2^{nd}, 3^{rd} and 4^{th} qualification flights, see Marcos, A. et al. (2015).

4. CONCLUSION

In this article, a methodological process to derive proper LFT models for the VEGA launcher during atmospheric flight has been presented. The proposed methodology was tailored to transfer the LFT modeling approach (and the associated robust μ analysis method) to the VEGA GNC group at ELV. Thus, emphasis was given to clearly present the modeling choices, its effects, the visualization of the simulation data, and the definition of the polynomial structures required for the LFT.

Although the LFT modeling and μ analysis approaches are not yet part of the official VEGA V&V process, the methodologies are been used routinely nowadays by the GNC group to increase their confidence on the tools and results.

REFERENCES

Balas, G.J., Doyle, J.C., Glover, K., Packard, A., and Smith, R. (1998). μ-Analysis and Synthesis Toolbox.

Charbonnel, C. (2010). H-infinity Controller Design and mu-analysis: Powerful Tools for Flexible Satellite Attitude Control. In *AIAA GNC Conference*. Toronto, Canada.

Doyle, J., Packard, A., and Zhou, K. (1991). Review of LFTs, LMIs, and μ. In *IEEE Conference on Decision and Contro*.

Ganet-Schoeller, M., Bourdon, J., and Gelly, G. (2009). Nonlinear and Robust Stability Analysis for ATV Rendezvous Control. In *AIAA GNC Conference*. Chicago, USA.

Jang, J.W., Van Tassell, C., Bedrossian, N., Hall, C., and Spanos, P. (2008). Evaluation of Ares I Control System Robustness to Uncertain Aerodynamics and Flex Dynamics. In *AIAA GNC Conference*. Honolulu, HA.

Lambrechts, P., Terlouw, J., Bennani, S., and Steinbuch, M. (1993). Parametric Uncertainty Modeling using LFTs. In *American Control Conference*, 267–272. San Franciso, CA.

Magni, J.F. (2004). Linear Fractional Representation Toolbox Modelling, Order Reduction, Gain Scheduling. Technical Report TR 6/08162 DCSD, ONERA, Systems Control and Flight Dynamics Department, Toulouse, France.

Marcos, A., Bates, D.G., and Postlethwaite, I. (2007). A Symbolic Matrix Decomposition Algorithm for Reduced Order Linear Fractional Transformation Modelling. *Automatica*, 43(7), 1125–1306.

Marcos, A., Bennani, S., and Roux, C. (2015). Stochastic mu-Analysis for launcher thrust vector control systems. In *CEAS GNC Conference*. Toulouse, FR.

Orr, J.S., Johnson, M.D., Wetherbee, J.D., and McDuffie, J.H. (2009). State Space Implementation of Linear Perturbation Dynamics Equations for Flexible Launcher Vehicles. In *AIAA GNC Conference*. Chicago, USA.

Pittet, C. and Arzelier, D. (2006). DEMETER: a benchmark for robust analysis and control of the attitude of flexible micro satellites. In *5th IFAC symposium on Robust Control Design - ROCOND 2006*. Toulouse, France.

Roux, C. and Cruciani, I. (2008). Scheduling Schemes and Control Law Robustness in atmospheric flight of VEGA. In *ESA GNC Conference*.

Szabo, Z., Marcos, A., Mostaza, D., Kerr, M., Rodonyi, G., Bokor, J., and Bennani, S. (2011). Development of an Integrated LPV/LFT Framework: Modeling and Data-Based Validation Tool. *IEEE Transactions on Control Systems Technology*, 19(1).